Self-Assembly in Mixtures of Poly(vinyl methyl ether) and Polystyrene-*block*-polyisoprene. 1. Formation of Nanocolloidal Spheres

Norio Iizuka,‡ Jeffrey Bodycomb,§ Hirokazu Hasegawa, and Takeji Hashimoto*

Department of Polymer Chemistry, Graduate School of Engineering, Kyoto University, Kyoto 606-8501, Japan

Received January 22, 1998; Revised Manuscript Received August 13, 1998

ABSTRACT: We studied phase behavior and molecular assembly in blends of poly(vinyl methyl ether) (PVME) and polystyrene-*block*-polyisoprene (SI) by small-angle X-ray scattering (SAXS), transmission electron microscopy (TEM), and light scattering. The neat block copolymer forms bcc (body centered cubic) spheres composed of polyisoprene block chains in a matrix of polystyrene block chains. On casting from a toluene solution, the blends with volume fractions of PVME less than or equal to 0.3 experienced only microphase separation, resulting in a structure with spherical microdomains of polyisoprene block chains (PI) in a matrix of polystyrene block (PS) chains (PS-corona) mixed with PVME, while the blends with volume fractions of PVME greater than 0.3 underwent macrophase separation into a PVME-rich region and an SI-rich region which was also microphase-separated. Furthermore, a thermoreversible one- to-two-phase transition induced by the change of segmental interactions between PS-corona and PVME was observed for the cast films. This system can be considered as a two-component system composed of nanocolloidal spheres of PI with PS-corona and PVME with a LCST phase diagram. The cloud point of the nanocolloidal spheres/PVME system is significantly lowered compared to that of a homopolystyrene/PVME blend due to the confinement of PS block chains onto the PI spheres. Note that the structures observed for this system are similar to those observed in colloidal dispersions of ionic latex particles in water and oil-in-water or water-in-oil microemulsions.

I. Introduction

Self-assembly, denoting the ordered structures and the ordering processes and mechanisms as a whole, in complex liquids or soft-condensed matter has been attracting much research interest as a problem related to nonlinear and nonequilibrium phenomena.[1,2] Along these lines, blends of two kinds of homopolymers A and B have been studied quite extensively.[3−7] Even for these simple blends the self-assembly behavior becomes quite complex but intriguing when the liquid−liquid-phase separation is coupled with other phase transitions such as those between liquid and solid (crystallization),[8,9] isotropic liquid and anisotropic liquid,[10−12] sol−gel transitions,[13] and so on, when at least one component is capable of undergoing such transitions on its own.

When these blends include a block copolymer, the phase separation of the system is also coupled with the behavior of the block copolymer. The block copolymer alone can undergo microphase separation and form microdomains with interesting structures such as lamella, strut (bicontinuous), cylinders on a hexagonal lattice, and spheres on a body centered cubic lattice (bcc).[14,15] This microphase separation can then be coupled with the macrophase separation between the diblock copolymer and another constituent of the blend (e.g., homopolymer) and therefore create a rich variety of patterns.[7,16−19]

For binary mixtures of a diblock and a homopolymer, much recent attention has been focused on systems of the type A−B/A where A−B is a diblock with one block consisting of monomers of type A and the other block of type B and where A is a homopolymer with monomers of type A (e.g., the repeat unit that is the same as that of the A block in A−B). This work has been directed toward research on miscibility or phase diagrams.[20−24] Furthermore, the effects of A on the concentration fluctuations in the single-phase state[17,25−30] and microphase transition,[17,21,27,28] on the size, morphology, and long-range order of these systems,[17,20,23,28,31−35] as well as on micelle formation[32,36−43] have been studied. Most of this research, however, has focused on the regime where only microphase separation takes place in the self-assembly process.

Another point that has been explored is the nature of the interaction between the homopolymer A and the A block of the diblock copolymer. It has been pointed out that in the case where the length of homopolymer A is equal to or greater than that of block A in the diblock, "dry brush" behavior is observed, where the homopolymer does not mix well with the similar block of the diblock. In the case where the A homopolymer is much shorter than the A block in the diblock, the system is observed to have "wet brush" behavior, where the homopolymer mixes well with the A block of the copolymer and influences the structure of the material.[33,35,44]

Here, we extend previous reports along these lines to blends of an A−B diblock with a third homopolymer C that is miscible with one block (A) but immiscible with the other block (B). Systems of the type A−B/C where C is a homopolymer different from either block A or block B of diblock A−B have only been recently examined. The self-assembly in the regime where both macrophase and microphase transitions take place has largely been ignored even for the case of A−B/A systems. For the A−B/C systems, there are a few isolated studies

* To whom correspondence should be addressed.
‡ Present address: Yarn Section, Toyobo Co., Ltd., Tsuruga Plant, Tsuruga, Japan.
§ Present address: Hashimoto Polymer Phasing Project, ERATO, JST, Keihanna Plaza, 1-7 Hikari Dai, Seika, Keihanna, Kyoto 619-0237 Japan.

10.1021/ma980084k CCC: $15.00
Published on Web 09/25/1998

Table 1. Polymers Used in This Work

sample code	sample	$M_n \times 10^{-4}$ [a]	M_w/M_n [b]	PS (wt %)	polymerization solvent	initiator
SI	polystyrene-*block*-polyisoprene	17.6	1.26	85	tetrahydrofuran	*sec*-butyllithium
HPS	polystyrene	20.4	1.06	100	benzene	*sec*-butyllithium
PVME	poly(vinyl methyl ether)	2.70	1.40	0	toluene	boron triflouride ethyl ether

[a] Membrane osmometry. [b] Size exclusion chromatography.

on the miscibility and the phase diagram.[18,45−52]

Kimishima et al.[53] examined the spatial distribution of poly(α-methyl styrene) in a blend of a polystyrene-*block*-polybutadiene-*block*-polystyrene triblock and poly(α-methyl styrene) and found that the poly(α-methyl styrene) tended to be solubilized in the center of the polystyrene (PS) domains compared with the case of blends of the same triblock with homopolystyrene (HPS).

Blends of poly(phenylene oxide) (PPO) and various triblock copolymers with one or two PS blocks have been examined previously by Tucker et al.[46−48] They reported an increase in solubilization of PPO in the PS block compared to the expected solubilization of HPS in the PS block of the triblock copolymers. They also noted that the effect of the homopolymer (PPO) molecular weight on its solubilization in the PS block was small or nonexistent. They ascribed both of these effects to the favorable interactions between the HPS and the PPO.[46−48] Hashimoto et al.[18] explored blends of polystyrene-*block*-polyisoprene diblock copolymers (SI) blended with PPO. They used differing solvent evaporation techniques to produce various self-assembled structures via control of both microphase and macrophase separation.[18] Lowenhaupt et al.[49] also pointed out that the attractive interactions between the homopolymer and one block of the diblock copolymer could suppress macrophase separation in blends of polystyrene-*block*-poly(methyl methacrylate) with such homopolymers as poly(cyclohexyl methacrylate), the polycarbonate of tetramethyl bisphenol A, or SAN (the azeotropic copolymer of styrene and acrylonitrile). All of these homopolymers are miscible with either PS or poly(methyl methacrylate) (PMMA) block chains. These blends are of the type A−B/C compared to blends of the type A−B/A. Recently, some further theoretical work has shown increased solubilization for a system where there are attractive interactions between the homopolymer and one block of the copolymer.[51] Also, the macrophase separation of polystyrene-*block*-polybutadiene (SB) blended with poly(vinyl methyl ether) (PVME) has been recently studied.[50] Finally, Lee et al. recently examined a blend of SI with PVME. They showed that the specific segmental interactions between the polystyrene block of the SI and PVME were important in controlling the behavior of these materials. They also explored the macrophase separation of these materials.[52]

In this paper, we investigate self-assembly in blends of polystyrene-*block*-polyisoprene (SI) and PVME. Blends of HPS and PVME are known to be miscible at low temperatures, but undergo a macrophase separation upon raising temperature (LCST behavior).[54−56] The SI diblock in this study is sufficiently long that it is microphase-separated at all accessible temperatures and has a composition such that it forms bcc spheres composed of block chains (PI) in the matrix of PS. Furthermore, we know that the miscibility of PS and PVME is driven by specific interactions between the PS and the PVME. The effect of these interactions on the behavior of diblock copolymer/homopolymer blends is a relevant question in the understanding of these materials. In the simpler case of the A−B/A type blend, we are concerned with only one Flory interaction parameter, $\chi_{A,B}$. However, here, we must consider interactions between the PS and the PI (within the diblock), $\chi_{S,I}$, interactions between the PS and the PVME, $\chi_{S,PVME}$, and finally, interactions between the PI and the PVME, $\chi_{I,PVME}$. Furthermore, since we will be casting these blends from a toluene solution, we will consider the χ values listed above as effective χ values in the medium of toluene. The χ values are therefore dependent on the concentration of toluene. Furthermore, with a change in temperature, χ also changes. As the values of the different χ values in the system vary, we observe either microphase or macrophase separation, leading to a rich variety of structures.

We can manipulate the self-assembly of the polymer structures via solution casting or annealing. In this work, we examine several issues that arise in considering the behavior of diblock copolymer and homopolymer blends: (1) the effect of solution casting versus annealing on the behavior of these blends, (2) the effect of chain confinement on the miscibility of PS block chains and PVME, and (3) the effect of specific segmental interactions on the self-assembly of these materials.

II. Experimental Methods

We used three polymers in this study, SI, PVME, and HPS, and tabulated their characteristics in Table 1. SI and HPS were prepared by living anionic polymerization and PVME by cationic polymerization. We have listed the initiators, solvents, and characterization techniques for each polymer in Table 1. Blends of SI and PVME with five different compositions (SI/PVME = 90/10, 70/30, 50/50, 30/70, and 10/90 vol %/vol %) were prepared by dissolving both polymers in toluene. Films of neat SI and SI/PVME blends were obtained by casting 10 wt % toluene solutions in Petri dishes at 30 °C. The solvent was evaporated over a period of two weeks, and then the film specimens were further dried under vacuum to constant weights at room temperature. Blends of HPS and PVME were also prepared in the same manner with six different compositions only for the purpose of cloud-point measurements.

The samples for the transmission electron microscope (TEM) were stained with osmium tetraoxide (OsO_4) vapor under the dry atmosphere and microtomed into ultrathin sections of about 50 nm thickness with an LKB Ultratome 4800A with a glass knife at room temperature. The ultrathin sections were floated on water and quickly transferred to a microscope grid coated with carbon film, and then stained again with OsO_4 vapor. OsO_4 is a selective staining agent for the polyisoprene blocks (PI), making the PI domains dark in the electron micrographs below. The ultrathin sections were then examined with a Hitachi H-600S transmission electron microscope operated at an accelerating voltage of 100 kV. Some samples (as described in the text) were further stained with 1% lead acetate aqueous solution, a staining agent for PVME. Neither of these staining agents stains the polystyrene blocks (PS).

Small-angle X-ray scattering (SAXS) was measured with an apparatus described elsewhere.[57−59] SAXS profiles were desmeared for slit width and slit height, and corrected for air scattering, absorption, and thermal diffuse scattering.[57−59]

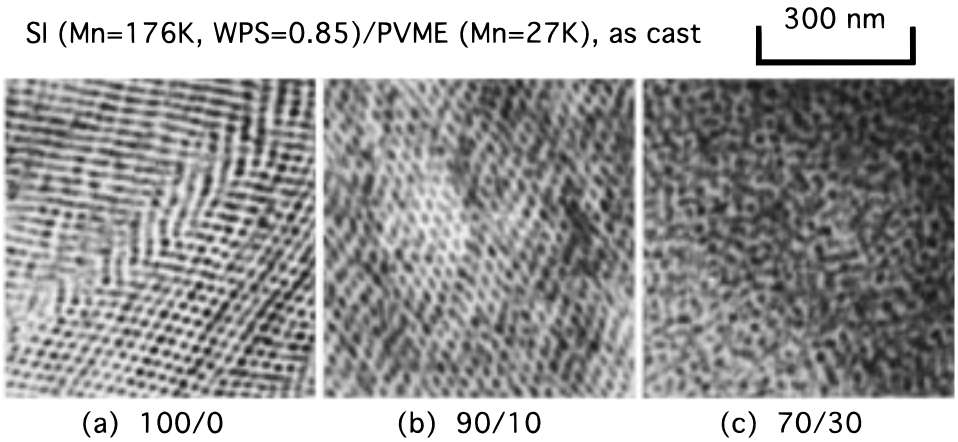

Figure 1. Transmission electron micrographs of OsO_4-stained ultrathin sections of SI/PVME blends cast from toluene solutions: (a)100/0, (b) 90/10, and (c)70/30 (vol %/vol %).

Light-scattering measurements were performed with a 15 mW He−Ne laser (wavelength 632.8 nm), with the incident beam perpendicular to the film surface, and recorded photographically or photometrically (for cloud-point measurements).

III. Results

III-A. Self-Assembly in the Solution-Cast Films. Self-assembling of the blends during the solution-casting process is an interesting subject to explore. Even by examining the structures in the solution-cast film, the self-assembling process may be conjectured.

First, the transparency of the as-cast blend films with various compositions was examined by eye, since macrophase-separated samples appear cloudy (or translucent) in general. When the volume fraction of PVME, ϕ_{PVME}, was >0.3, the as-cast films were translucent, suggesting macrophase separation between SI and PVME, while they were clear when $\phi_{PVME} \leq 0.3$, suggesting no macrophase separation. SAXS measurements on the as-cast films indicated that in all cases they contained a microphase-separated structure of spherical microdomains arranged on a bcc lattice.

Figures 1 and 2 show the TEM micrographs of the as-cast films stained by OsO_4. As shown in Figure 1, the optically transparent as-cast films with $\phi_{PVME} \leq 0.3$ (100/0, 90/10, and 70/30) all show a uniform structure composed of the dark spheres with a diameter of about 20 nm corresponding to PI microdomains and the bright matrix of unstained PS and PVME which are probably mixed in the segmental level. These results match those of the optical observations tabulated in Table 2. Thus, the as-cast films with $\phi_{PVME} \leq 0.3$ form a single-phase mixture of SI and PVME with PI blocks forming spherical microdomains uniformly distributed in the matrix composed of PS blocks and PVME.

On the other hand, the 50/50 as-cast film ($\phi_{PVME} = 0.5$) has a nonuniform structure consisting of the bright droplets of about 1 μm and the dark background as shown in Figure 2 taken with a lower magnification than Figure 1, suggesting the macrophase separation. The inset of Figure 2 is a blowup of the dark background which clearly shows the dark spheres in the bright matrix and resembles the structures shown in Figure 1. In contrast, dark spheres are not observed in the bright droplets. Most of the droplets have holes while some of them do not. The holes may have been formed during microtoming or floating on water. The ellipsoidal shape and anisotropic orientation of the droplets probably resulted from the deformation of the sample specimen during the ultra-microtoming. The droplets are supposed to be originally spherical in the cast film, but they must have been squeezed to have the oval shapes on cutting in such a way that their short axes are parallel to the cutting direction. This evidence suggests that the bright droplets are composed of PVME-rich phase while the dark matrix is composed of SI-rich phase. The PVME-rich droplets are above the glass-transition temperature ($T_g = -27$ °C) at room temperature and ready to deform on cutting, while the PI spherical microdomains are fixed by OsO_4 and stable for deformation. In addition, PVME is soluble in water. The volume fraction of the PVME-rich droplets in Figure 2 is much smaller than 0.5, suggesting that a significant amount of PVME is still mixed with PS in the dark matrix.

Figure 3 shows an optical micrograph of the 50/50 as-cast film. We can clearly see that the system shows a two-phase structure with a fairly uniform spacing of 2−3 μm. Also, it appears as if both phases are co-continuous, which is in conflict with the TEM results. However, this could be indicative of spinodal decomposition between SI and PVME during the solvent evaporation.[60] The droplets are small compared to the focal depth of the optical microscope we used, and they are observed to overlap each other in the optical micrograph shown in Figure 3. If the spatial arrangement of the droplets reflects the memory of the co-continuous structure previously formed during spinodal decomposition before the occurrence of the percolation-cluster transition, the images of the overlapped PVME-rich droplets may appear as a co-continuous structure in the optical micrograph.[61] This suggestion of a co-continuous structure formed during the casting process indicates that the phase-separated structure formed via spinodal decomposition. The percolation-cluster transition should occur due to the asymmetric volume fractions for SI-rich and PVME-rich phases as observed by TEM in Figure 2.

Figure 4 shows the light-scattering pattern from the 50/50 as-cast film. As we expect from the optical micrograph showing a uniform spacing in Figure 3, we see a spinodal ring for the as-cast system, indicating that the system underwent spinodal decomposition during the solvent evaporation process. The spinodal ring has a maximum intensity at the scattering vector $q_m \cong 1.4\ \mu m^{-1}$ which indicates the characteristic length (Λ_m) of the concentration fluctuations $\Lambda_m = 2\pi/q_m \cong 4.5$

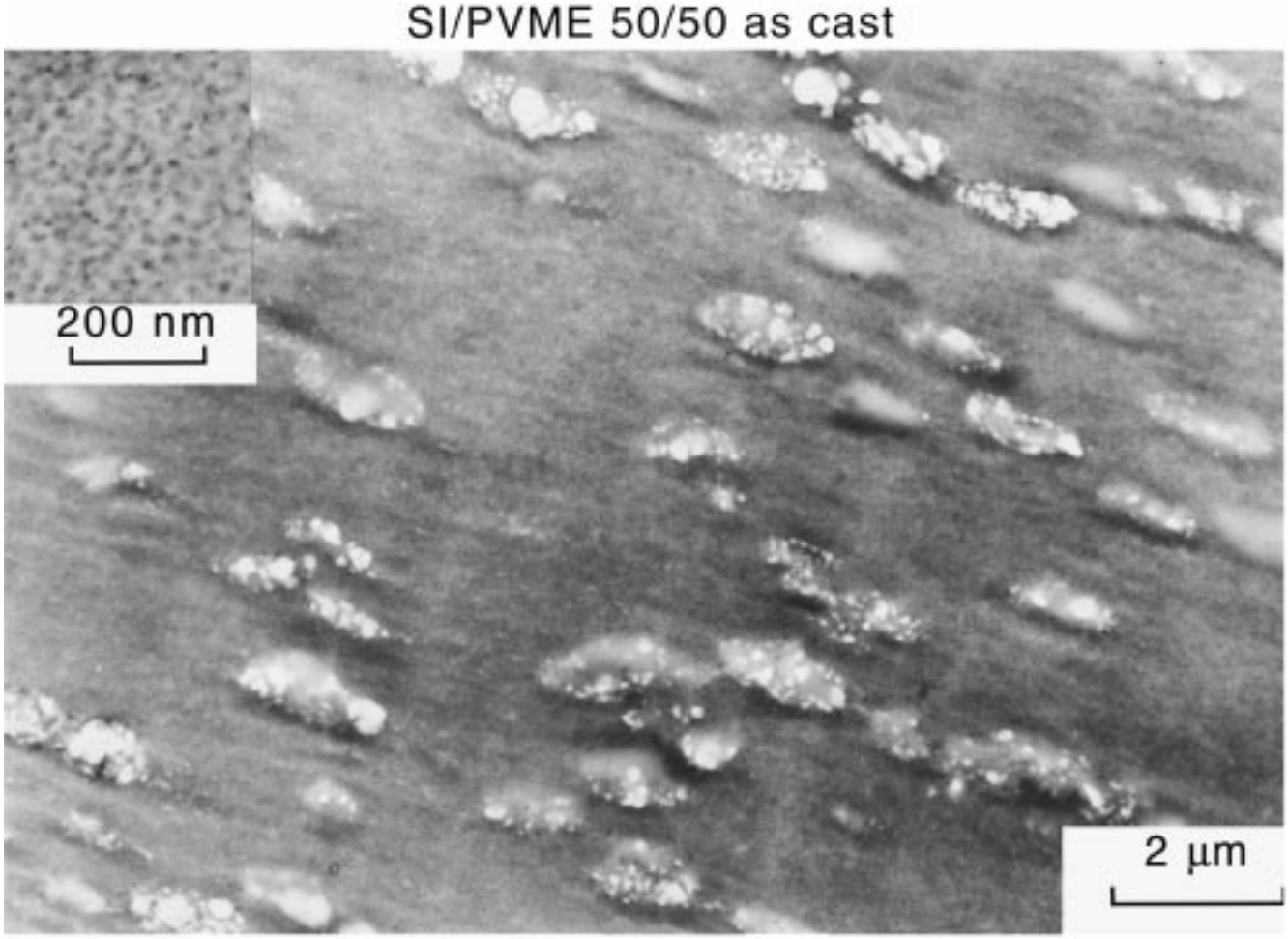

Figure 2. Low-magnification and high-magnification (inset) transmission electron micrographs of OsO_4-stained ultrathin sections of 50/50 (vol %/vol %) SI/PVME blend.

Table 2. Summary of Blend Characteristics for SI/PVME As-Cast Films

SI/PVME (vol/vol)	transparency of as-cast sample	microdomain morphology[a]	remarks
100/0	clear	PI spheres bcc	single phase
90/10	clear	PI spheres bcc	single phase
70/30	clear	PI spheres bcc	single phase
50/50	translucent	PI spheres (bcc in SI-rich domain)	two phase
30/70	translucent	PI spheres (bcc in SI-rich domain)	two phase

[a] By SAXS and TEM.

μm. (The scattering vector, q, is defined by $q = (4\pi/\lambda)\sin(\theta/2)$ where λ and θ are the wavelength of the light and the scattering angle in the sample, respectively.) This value is twice as large as that obtained from the optical micrograph in Figure 3. In the optical micrograph the structures are overlapped in the depth direction and the observed spacing becomes smaller than the real one.

To summarize the above results, the as-cast films have the single-phase or two-phase structure depending on the blend composition. When $\phi_{PVME} \leq 0.3$, SI is mixed with PVME and when $\phi_{PVME} > 0.3$, SI and PVME are macrophase-separated. However, in both cases PI block chains are microphase-separated to form spherical microdomains arranged on a cubic lattice in a matrix of PS block chains and PVME in the SI-rich phase.

III-B. Effects of Thermal Treatment. We used light scattering to examine the effect of thermal treatment on the behavior of the 50/50 blend of SI/PVME. The light-scattering pattern from the as-cast specimen exhibiting a spinodal ring is shown in Figure 5a again. After annealing the specimen at 100 °C for a few hours, the spinodal ring disappears as shown in Figure 5b (the scattering near the beam stop is actually part of the incident beam) indicating a single-phase system, that is, PVME in the droplets as shown in Figure 2 was mixed with the PS blocks and the PI spheres were uniformly distributed in the matrix of PS and PVME. This shows that the as-cast film does not have an equilibrium structure and that the equilibrium structure below 100 °C is the single-phase structure. Finally, upon annealing at 140 °C for 5 min, we obtain Figure 5c, a system that is again macrophase-separated. We can go from Figure 5c to Figure 5b by annealing again at 100 °C, showing a thermoreversible structure change. Thus, this system shows a reversible transition: macrophase separation via spinodal decomposition on annealing at 140 °C and phase-mixing on annealing at 100 °C. In a companion paper, the kinetics of the phase behavior of this sample will be discussed.[62]

Figure 6 shows the TEM micrograph of the 50/50 blend macrophase-separated via spinodal decomposition by annealing at 140 °C. In this case the translucent as-cast sample was first annealed at 110 °C, which clarified the sample to form the single-phase structure composed of PI spheres in a matrix of PS and PVME,

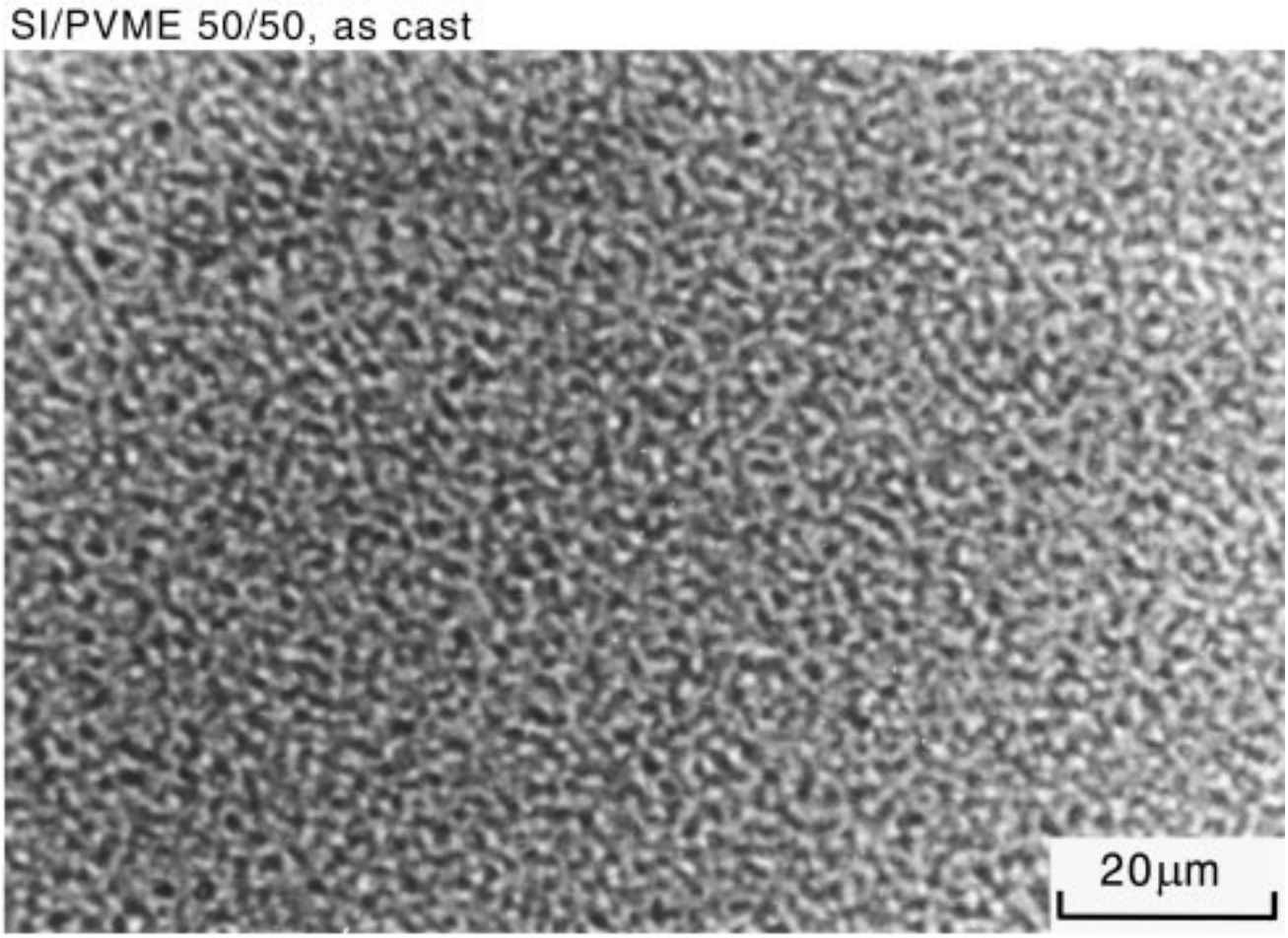

Figure 3. Transmission optical micrograph of 50/50 (vol %/vol %) blend of SI/PVME blend cast from a toluene solution.

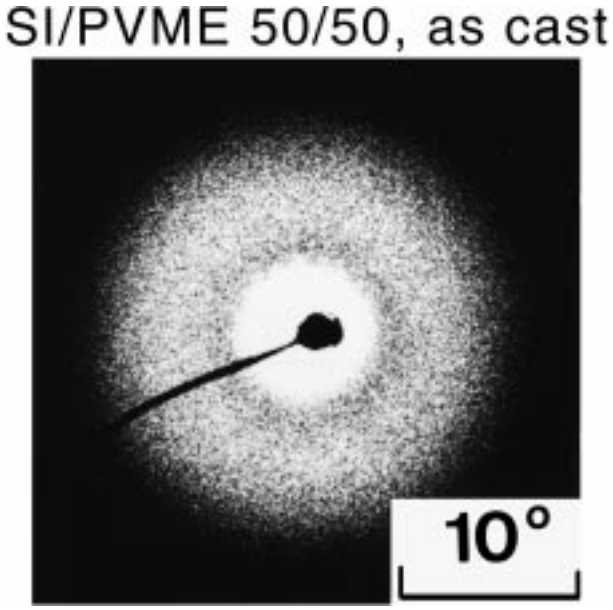

Figure 4. Light-scattering pattern of 50/50 (vol %/vol %) blend of SI/PVME blend film cast from a toluene solution.

then annealed at 140 °C for 1 h, which generates the macrophase-separated structure via spinodal decomposition, and then quenched to preserve the structure. Since the ultrathin section was stained first with OsO_4 and subsequently with lead acetate which selectively stains PVME, both PI and PVME phases appear dark in the micrograph. In Figure 6, we see the structure similar to Figure 2, that is, the SI-rich regions as the PI spheres (which we will call "nanocolloidal spheres" because their radii are about 12 nm) uniformly dispersed in the PS matrix mixed with a certain amount of PVME and large dark droplets of PVME-rich regions. The dark droplets having a size on the order of 500 nm correspond to the bright regions observed in Figure 2, but since they are stained with lead acetate, they have become dark and we can conclude that they are PVME. The black spots with variable sizes on the PVME droplets are the lead acetate particles that remained on the section without being washed out. Therefore, the PVME droplets hardly contain the nanocolloidal spheres. Furthermore, we can conclude that the macrophase separation observed by light scattering corresponds to a phase separation between the nanocolloidal spheres and the PVME through the segmental interactions between PS blocks attached to the spheres and the PVME.

Figure 7 shows the results of SAXS measurements on these blends with various compositions annealed at 100 °C for a sufficiently long time that the systems have the single phase of nanocolloidal spheres (or the structure that is only microphase-separated, but not macrophase-separated). The data points are marked by the symbols, and the solid lines indicate the results from paracrystalline analysis.[63,64] In all cases the system behaves as spheres on a bcc lattice with the lattice-scattering peaks at the relative positions 1, $\sqrt{2}$, and $\sqrt{3}$ as indicated by thin arrows. The particle-scattering peaks by the spherical microdomains are indicated by

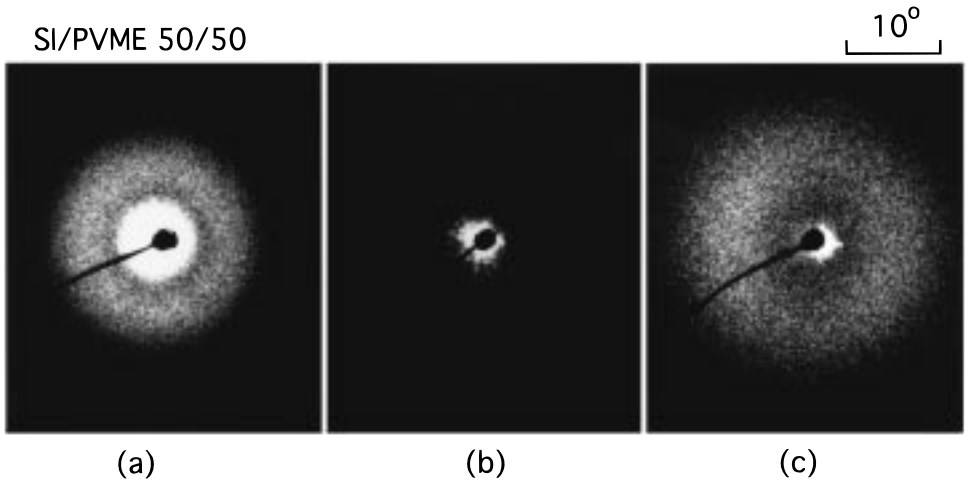

Figure 5. Light-scattering pattern of 50/50 (vol %/vol %) blend of SI/PVME blend cast from a toluene solution (a) as-cast, (b) after annealing at 100 °C for about 12 h, and (c) after annealing at 140 °C for 5 min and quenching to room temperature.

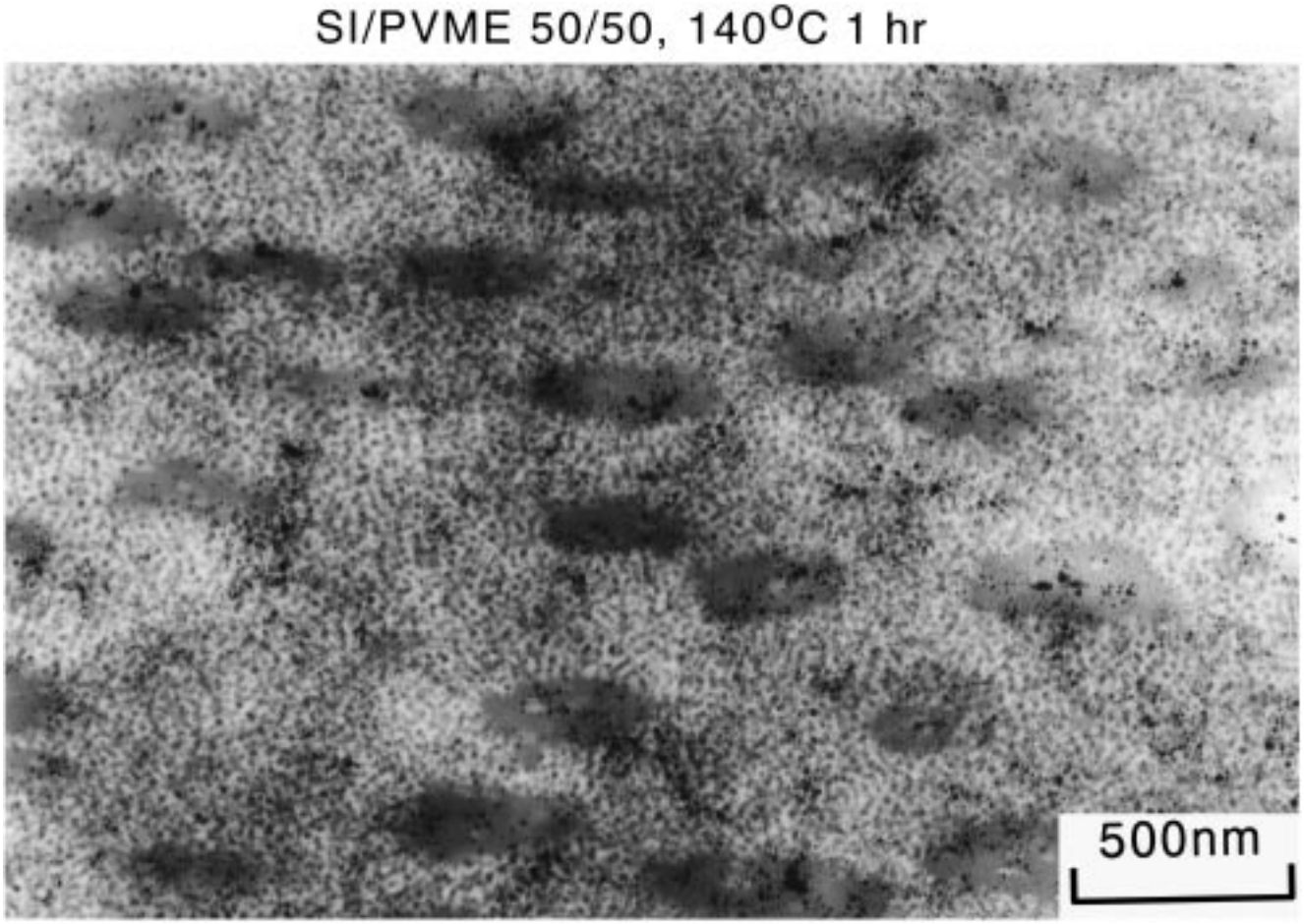

Figure 6. Transmission electron micrographs of OsO_4- and lead acetate-stained ultrathin sections of SI/PVME 50/50 (vol %/vol %) blend of SI/PVME blend cast from a toluene solution after annealing at 140 °C for 1 h and quenching to room temperature.

thick arrows. We have tabulated the results of the paracrystalline analysis in Table 3. We should point out that the most important parameters for our discussion, D (the shortest or nearest-neighbor intersphere distance in bcc) and R (the radius of the polyisoprene spheres), can also be obtained from simply examining the first-order scattering peak from the cubic lattice and from the form factor of a single PI sphere, respectively, if the symmetry of the cubic lattice is sufficiently high and the size distribution of the spheres is sufficiently narrow. However, paracrystalline analysis allows us to use the whole scattering profile so that it quantitatively identifies the symmetry of the cubic lattice and determines lattice parameters, the average size of the spheres, the lattice distortion, the size distribution of the spheres, etc., in good accuracy. Below, we will use these results to discuss in further detail the interactions between the PS and the PVME as well as the PI and the PVME.

From the small-angle scattering peaks at $q \leq 0.12$ nm^{-1} which arise from intersphere interference of the scattered waves (as indicated by the arrows marked by

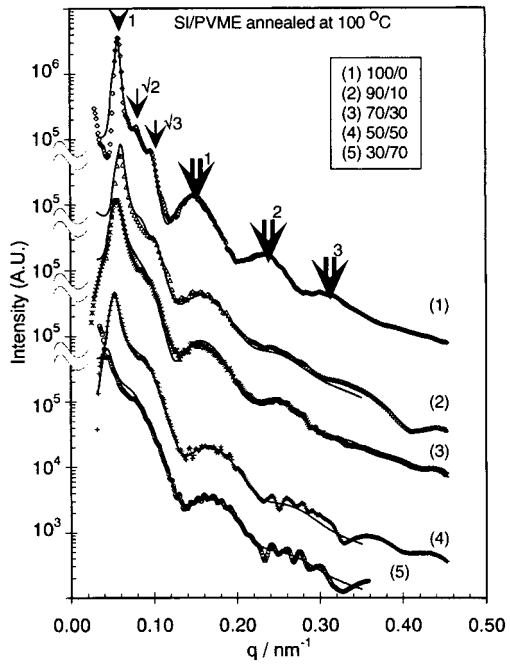

Figure 7. SAXS profiles of SI/PVME blends cast from toluene solutions and annealed at 100 °C for about 12 h. The solid lines show the best-fit theoretical profiles obtained from a paracrystalline model.

1, $\sqrt{2}$, and $\sqrt{3}$), we obtain information about the lattice symmetry (in this case, bcc) and the domain spacing, from which we obtain the nearest-neighbor distance, D. From the relative heights of the peaks, as well as their widths, we determine the volume fraction of the PI spheres and the paracrystalline distortion factor, g. From the multiple peaks attributed to the form factor of PI spheres as indicated by the thick arrows marked by 1, 2, and 3, we determine the average radius of the PI spheres and the distribution of the radii. Thus, we have used the whole scattering curve in calculating these parameters with higher accuracy. Table 3 reveals the following: The paracrystalline distortion factor, g, increases with increasing volume fraction PVME, which suggests that the bcc lattice becomes somewhat less ordered with increasing PVME, except for $\phi_{PVME} = 0.3$. The width of the distribution of radii of the PI spheres, σ_R, also increases. Both of these trends can be explained if one considers that the local concentration fluctuations of the PVME homopolymer between the nanocolloidal spheres increase with increasing ϕ_{PVME} in the blends since the PVME homopolymer has considerable freedom to rearrange itself.

Upon summarizing the results shown in Figures 5−7, which were obtained after annealing and are therefore free from the history of solution casting, we have the following picture for the self-assembly of the bulk SI/PVME systems. At lower temperatures (e.g., at 100 °C) the systems form a single mesophase of nanocolloidal spheres on a bcc lattice as schematically shown in Figure 8a. At higher temperatures (e.g., at 140 °C) the systems form a two-phase structure in which the regions rich in SI and poor in PVME (Figure 8b) coexist with the regions poor in SI and rich in PVME (Figure 8c). The local concentration of PVME in the regions rich in SI (Figure 8b) is much smaller than that of the PVME in the single-phase state (Figure 8a), so that the intersphere distance, D, of the former is smaller than that of the latter (defined hereafter as D_0). The SAXS data showed that the regions rich in SI also form a bcc structure, although they are not shown here. In the PVME-rich region the PI spheres may only have short-range liquidlike order.

Finally, we can determine a phase diagram for the nanocolloidal systems and use this system in order to examine the effect of chain confinement on the phase diagram between PS and PVME. We performed cloud-point measurements by light scattering on the SI/PVME blends undergoing a phase transition between the single-phase state (Figure 8a) and the two-phase state (Figures 8b and 8c), and on the blends of homopolystyrene (HPS) and the same PVME for comparison. The results are shown in Figure 9. The following two scales are attached to the abscissa: the volume fraction of PVME in the SI/PVME blends (the upper abscissa scale), $\phi_{PVME,SI/PVME}$, and the volume fraction of PVME in the mixture of PS (corona or homopolymer) and PVME, referred to the SI/PVME blends or to the HPS/PVME blends (the lower abscissa scale), $\phi_{PVME}/(\phi_{PS} + \phi_{PVME})$.

The HPS/PVME and SI/PVME blends are in a single-phase state and a two-phase state below and above the corresponding cloud-point curve, respectively. The SI/PVME blends form the state schematically shown in Figure 8a in the single-phase state below the cloud-point curve where the PS-corona is mixed with PVME. In the two-phase state above the cloud-point curve, they form the state schematically shown in Figures 8, parts b and c, where PVME tends to phase-separate from the PS-corona, hence giving rise to the two-phase coexistence. From these measurements, we can see that the nanocolloidal spheres with PS-corona/PVME blend phase separate at a lower temperature than the HPS/PVME blend even though the molecular weight of HPS is much higher than that of the PS blocks of SI. Thus the PS-corona (the PS chain confined to the surface of the PI spheres) is less miscible with the PVME than the HPS is (free, unconfined HPS chains), consistent with our earlier results.[33,50]

IV. Discussion

The structures investigated in this work are nanocolloidal spheres of PI with PS-corona chains in a matrix of PVME. There are four main results from this work: (i) We can use both solution casting and thermal treatment to manipulate the ordered structure of diblock copolymer/homopolymer blends. (ii) Segmental interactions between the PVME and PS block of the diblock copolymer control miscibility between the nanocolloidal spheres and the PVME and change the behavior of the corona PS chains from that of dry-brush to wet-brush behavior or vice versa against PVME. (iii) Chain confinement enhances the demixing of the nanocolloidal spheres/PVME blends relative to the demixing of the HPS/PVME blends. (iv) There is an interesting parallel between the behavior of this system and some observations on colloidal particles in solution and on micellar solutions in microemulsions. These are discussed in detail below.

IV-A. Solution-Casting Process and Thermal Treatment. We can control the polymer structure through two methods: the use of solution casting and thermal treatment. Figure 10 shows a schematic of the relevant phase diagram which we can use to illustrate the two representative paths, 1 and 2, in the solvent evaporation process at a particular temperature. The

Table 3. Results of Paracrystalline Analysis on Blends[a]

ϕ_{PVME}	lattice	a (nm)	R_{PI} (nm)	σ_R (nm)	D (nm)	$\phi_{PI,comp}$	$\phi_{PI,SAXS}$	n	g	a_j (nm)
0.0	bcc	48.9	12.6	1.00	42.3	0.170	0.143	177	0.10	3.36
0.1	bcc	46.0	11.7	1.40	39.8	0.153	0.138	142	0.12	3.49
0.3	bcc	49.2	11.8	1.10	42.6	0.119	0.116	145	0.16	3.47
0.5	bcc	52.6	11.1	1.30	45.6	0.085	0.079	121	0.14	3.58
0.7	bcc	62.0	11.2	1.40	53.7	0.051	0.049	124	0.18	3.56

[a] ϕ_{PVME}, volume fraction PVME in the blends; a, edge length of bcc cell; R_{PI}, average radius of PI spheres; σ_R, standard deviation of distribution of radii of PI spheres; D, distance between the nearest spheres in bcc lattice; $\phi_{PI,comp}$, volume fraction of PI spheres calculated from composition of the blend on the basis of the assumption of complete phase separation of PI blocks from PS blocks and PVME; $\phi_{PI,SAXS}$, volume fraction of PI spheres calculated from the SAXS results on a and R_{PI}; n, number of block copolymer chains per sphere; g, paracrystalline distortion factor (root-mean-square deviation of D divided by the mean value of D); a_j, average nearest-neighbor distance between chemical junctions of SI at the interface.

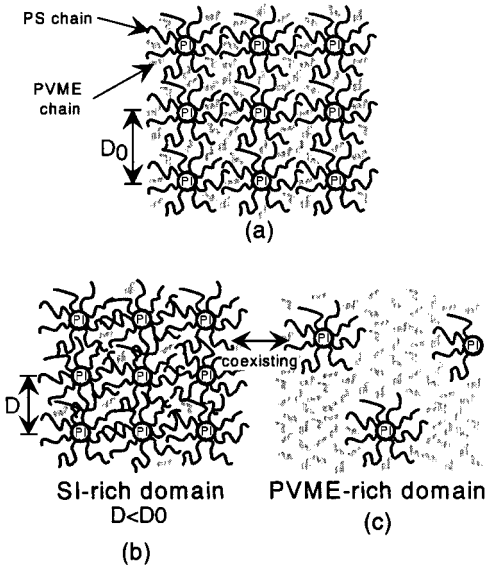

Figure 8. Schematic of the structure of SI/PVME blend: (a) low temperature, single phase, (b) high temperature (macrophase-separated), SI-rich phase (left), and (c) SI-poor phase (right).

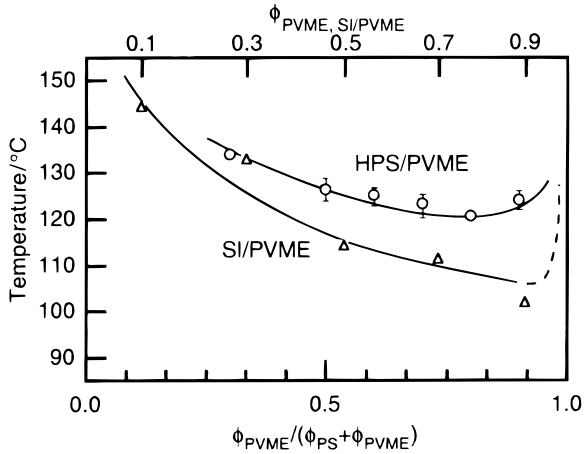

Figure 9. Experimental cloud-point curves for the SI/PVME and HPS/PVME blends, where two kinds of abscissa were used: $\phi_{PVME}/(\phi_{PS}+\phi_{PVME})$ refers to the volume fraction of PVME in the mixture of PVME and PS (corona for the SI/PVME blend and homopolymer for the HPS/PVME blends) and $\phi_{PVME,SI/PVME}$ refers to the volume fraction of PVME in the SI/PVME blends.

curves a and b schematically illustrate the phase boundaries for the microphase separation of SI in the SI/PVME/toluene system and the macrophase separation between the PVME and the disordered SI in toluene, respectively. It should be noted that both curve a and curve b do not exist in a ternary system of HPS/PVME/toluene at low temperatures. Curve b exists in

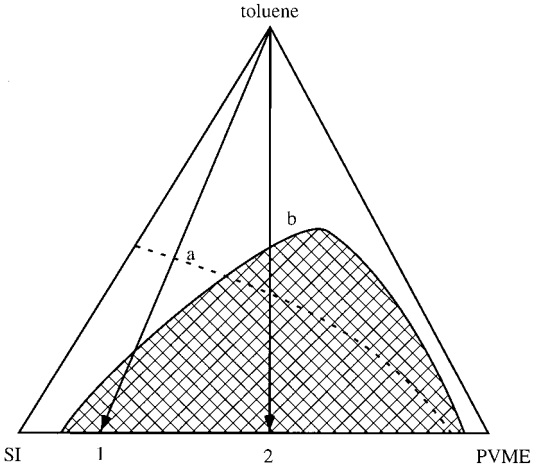

Figure 10. Schematic ternary phase diagram of SI/PVME/toluene at a given temperature. Curves a and b schematically represent the stability limit for the microphase separation of SI and that for the macrophase separation between PVME and disordered SI, respectively.

the SI/PVME/toluene system where SI is in a disordered state because of the repulsive interaction between the PI block and the PVME.[65] The shapes and the relative heights of curves a and b in the triangular phase diagram depend on the molecular weight of SI and PVME as well as on the composition of the SI diblock copolymer, and the curves shown here are just schematic. In Figure 10, we have a three-component system of SI, toluene, and PVME (here we shall consider SI as a single component regardless of its being ordered or disordered).

On solution casting, we remove the toluene from the solution at a constant temperature, traveling along a line from near the top vertex (close to 100% toluene) to the base of the triangle in Figure 10. If we travel along line 1, where the PVME is less than or equal to 30% of the polymer in the system, we encounter curve a (microphase separation) first, and later curve b (macrophase separation). However, if the microphase separation occurs first, curve b for the macrophase separation between disordered SI and PVME (not for the macrophase separation between ordered SI, i.e., PI spheres with PS-corona and PVME) loses its physical significance and the final structure will be more or less affected by the microphase separation because the repulsive interaction between the PI blocks and the PVME is shielded by the PS blocks. If we travel along line 2, where the PVME is greater than 30% of the polymer in the system, we encounter macrophase separation first, which develops phases rich in SI and PVME, and then microphase separation occurs in the phase rich in SI on further increases of polymer concentration,

leading to a two-phase structure. Thus, we arrive at the base of the triangle (solvent-free system) with two completely different polymer structures depending on whether the system underwent microphase or macrophase separation first. Since the casting was done at 30 °C, as the toluene leaves the system, the structure essentially vitrifies when the glass-transition temperature of the PS-rich phase becomes close to the casting temperature.

Once the samples have been cast into films and dried completely, the phase diagram of the two-component system composed of the nanocolloidal spheres of PI with PS-corona and PVME may apply. This phase diagram can be represented by the LCST cloud-point curve of SI/PVME shown in Figure 9. Since the order−disorder transition (ODT) temperature of the nanocolloidal spheres is far above the thermal degradation temperature of the SI diblock copolymer, we can consider the nanocolloidal spheres as one component in the accessible temperature region. It should be noted that, in this phase diagram, only the LCST phase boundary exists and the phase boundary such as curve b considered in Figure 10 no longer exists, since the PI blocks are essentially shielded by the PS-corona and there is no direct interaction between the PI and PVME segments.

As we anneal the as-cast films of the SI/PVME blends above the T_g of the PS-corona mixed with some PVME but below the LCST, the systems are no longer frozen and they achieve thermodynamic equilibrium to form the single phase composed of the nanocolloidal spheres and PVME. On further heating the 50/50 blend at 140 °C, which is far above its LCST, the PVME and the nanocolloidal spheres demix by spinodal decomposition, giving the two-phase structure as shown in Figure 6 and the spinodal ring as shown in Figure 5.

Thus, two different approaches, solution casting and thermal treatment, are possible to control the self-assembly of SI/PVME. By solution casting, a nonequilibrium structure that shows microphase as well as macrophase separation or an equilibrium structure that only shows microphase separation can be obtained depending on the blend composition. The spatial distribution of the nanocolloidal spheres of SI in a matrix of PVME can be controlled by annealing at different temperatures.

IV-B. Wet-Brush and Dry-Brush Behavior. Now we would like to compare the SI/PVME system with SI/homopolystyrene (HPS) systems from the viewpoint of the wet-brush/dry-brush behavior. In general, diblock copolymer (e.g., A−B)/homopolymer (e.g., A) blends have been shown to have different behavior depending on the relative molecular weight of the homopolymer A compared to the molecular weight of the similar block A of the diblock copolymer A−B. It has been shown that when the homopolymer is longer than the similar block of the diblock, dry brush behavior is observed, and when it is shorter, wet-brush behavior is observed.[33,35,44] It would be useful to be able to manipulate this behavior by changing some parameter (such as Flory interaction parameter χ) other than the molecular weight. For an A−B/A blend, χ parameter between homopolymer A and A block is 0 regardless of temperature, while χ parameter changes with temperature for an A−B/homopolymer C blend such as $\chi_{S,PVME}$ for the SI/PVME blends. With the results of this study, we can check the viability of using the temperature dependence of $\chi_{S,PVME}$ to change the regime of wet-brush and dry-brush behavior.

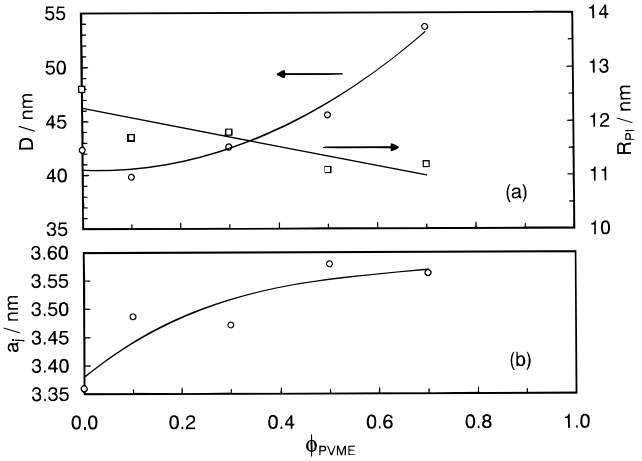

Figure 11. (a) The nearest interdomain distance in bcc, D, and radius of PI spheres (R_{PI}), and (b) average distance between chain junctions along the interface as a function of the volume fraction of PVME, ϕ_{PVME}, all of which are determined from SAXS with the samples annealed at 100 °C.

The PVME chains are much shorter than the PS block of the SI, suggesting wet-brush behavior even when $\chi_{S,PVME} \cong 0$ as in the case of PS and HPS in SI/HPS blends.[33,35,44] However, there are specific segmental interactions between the PS and the PVME in this system, which makes $\chi_{S,PVME} < 0$ at temperatures lower than a characteristic temperature. If $\chi_{S,PVME} < 0$, the system should show this behavior even more strongly than the case of $\chi_{S,PVME} \cong 0$. With increasing temperature, however, $\chi_{S,PVME}$ changes from negative to positive. If $\chi_{S,PVME}$ becomes a large positive value, even the short PVME chain is expected to display dry-brush behavior. We can use the SAXS data to characterize the degree of interpenetration between the PVME and the PS block and to explore whether the change of $\chi_{S,PVME}$ with temperature causes a wet-brush to dry-brush transition with temperature.

In Figure 7, we showed the results of SAXS measurements on the various blends after annealing at 100°C for a couple of hours, thus having a single-phase structure. Figure 11 summarizes the results of the SAXS analysis (Table 3). We see that the interdomain distance, D, is a weak function of the volume fraction of PVME, ϕ_{PVME}, in Figure 11a. It increases from about 40 to 55 nm on the addition of PVME. The mean radius of the spheres, R_{PI}, decreases with ϕ_{PVME} as shown in Figure 11a, indicating that the average distance, a_j, between junctions of the PS and PI blocks at the interface is increasing, as shown in Figure 11b. This is a clear indication of wet-brush behavior even at 100 °C which is very close to the LCST. Dry-brush behavior would be characterized by a constant a_j.[33,35,44] Therefore, these SAXS results show that specific PS/PVME segmental interactions lead to well-expected wet-brush behavior. Upon further raising the temperature, the system eventually phase-separates above 140 °C as shown in Figure 8, indicating clearly that PS/PVME segmental interactions lead to dry-brush behavior at these temperatures.

We can also use the SAXS data to check whether there is complete segregation of the PI blocks from the matrix phase composed of PS blocks and PVME. In Figure 12, we show the volume fraction of PI spheres, ϕ_{PI}, calculated from the SAXS data (circles) obtained from the samples annealed at 100 °C as well as the calculated result from assuming complete segregation

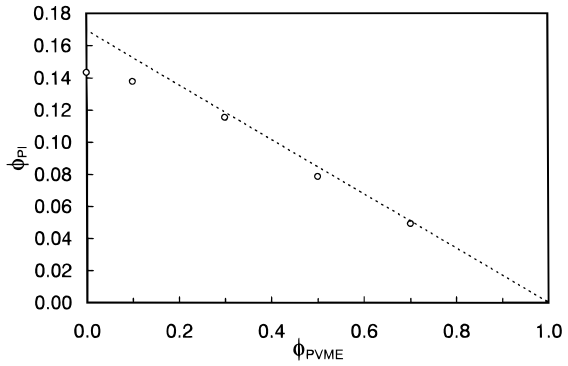

Figure 12. Volume fraction of polyisoprene spheres, ϕ_{PI}, against volume fraction of PVME, ϕ_{PVME}, as determined by SAXS (circles) compared with that based on stoichiometric calculation for the case of complete segregation (broken line).

(broken line). We see that, upon addition of PVME, the volume fraction of PI spheres closely follows that assumed by complete segregation, suggesting that the PVME is not swelling the PI spheres and remains only in the PS matrix and that few PI block chains are solubilized in the matrix of PS and PVME. We speculate that the deviations of the two results observed for a small value of PVME arise from a nonequilibrium effect: the blends with a low content of PVME have a relatively high glass-transition temperature of the PS phase so that the mobility of the nanocolloids is relatively low. Therefore, the annealing may not be sufficiently long for these systems.

IV-C. Effect of Chain Confinement. From the cloud-point curves, we can comment on the effect of confinement of PS on the miscibility of PS with PVME. For the case of diblocks, one end of the PS blocks is confined to the surface of PI spheres, as they must be attached to the PI, which is on the other side of the interface in the microphase-separated domains. However, in the case of HPS/PVME blend, the polystyrene is allowed to move freely. Thus, we see that, by confining the chains, we have lowered the phase separation temperature of a LCST system, or destabilized the single phase. Such an effect has also been observed for polystyrene-*block*-polybutadiene (SB)/PVME blends.[50] Also, Lee et al. showed that a higher molecular weight diblock SI blended with PVME had a higher cloud point than a blend of PVME with a lower molecular weight diblock and explained their results in terms of chain confinement.[52]

IV-D. Comparison with Other Systems. Finally, there is an interesting parallel between our structure and that seen in "classic" colloidal systems. Ise et al. have published extensive work showing that ionic latex spheres in water form a "two-state" structure in which the sphere-rich regions coexist with sphere-poor regions.[66] In this case, we observe a collection of PI spheres with PS-coronal chains (nanocolloidal spheres) in an isotropic matrix (PVME). Thus we can regard the nanocolloidal spheres as similar to the latex particles, and the PVME as a solvent, much like the water in Ise's system. However, it should be pointed out that the nature of the interaction is dramatically different, as in this case there are no ionic interactions as seen in the case of ionic latex spheres in water. In our system the origin of the net attractive or repulsive interactions between colloids is clearly related to the net segmental interactions between the PS-corona and the PVME homopolymer. Furthermore, an intriguing analogy also exists between our structure and oil-in-water (or water-in-oil) microemulsion systems composed of water, oil, and a surfactant.[67−69] A microemulsion with a given set of components shows a single-phase micellar solution or a two-phase micellar solution in which micellar-rich and micellar-poor phases coexist, depending on thermodynamic variables such as temperature and pressure. The similarity in the structure of this system and other systems suggests the possibility that there are similarities in the self-assembly of these systems, though the nature of the interactions as well as the time and length scales of organization may be widely different, which merits further investigation.

V. Conclusion

We can manipulate the structure of SI/PVME systems by using both the solution-casting process and thermal treatment. Furthermore, we can use temperature to vary specific segmental interactions and therefore change the system between that showing dry-brush behavior and that showing wet-brush behavior. In addition, we have been able to determine a phase diagram for nanocolloidal spheres of PI with PS-coronal chains with PVME and to show that confinement of the polystyrene blocks to PI spheres causes the polystyrene/PVME system to demix at lower temperatures. Finally, we note that the structures observed here are similar to those observed in ionic colloidal systems of latex in water and micellar solutions in microemulsons, and hence call this structure "nanocolloidal spheres".

Acknowledgment. This work has been supported by a Grant-in-Aid for Priority Areas, "Phase Transformation" from the Ministry of Education, Science, Culture, and Sports, Japan (10136223).

References and Notes

(1) Komura, S., Furukawa, H., Eds. *Dynamics of Ordering Processes in Condensed Matter*; Plenum Press: New York, 1988.
(2) Onuki, A., Kawasaki, K., Eds. *Dynamics and Patterns in Complex Fluids*; Springer-Verlag: Berlin, Germany, 1990.
(3) Nose, T. *Phase Transitions* **1987**, *8*, 245.
(4) Hashimoto, T. *Phase Transitions* **1988**, *12*, 47.
(5) Takenaka, M.; Tanaka, K.; Hashimoto, T. In *Contemporary Topics in Polymer Science, Vol. 6, on Multiphase Macromolecular Systems Symposium*; Culbertson, W. M., Ed.; Plenum Press: New York, 1989; p 363.
(6) Utracki, L. A. *Polymer Alloys and Blends*; Hanser: Munich, Germany, 1990.
(7) Hashimoto, T. In *Structure and Properties of Polymers*; Cahn, R. W., Haasen, P., Kramer, E. J., Eds.; Materials Science and Technology, Vol. 12; VCH: Weinheim, Germany, 1993; p 251.
(8) Inaba, N.; Sato, K.; Suzuki, S.; Hashimoto, T. *Macromolecules* **1986**, *19*, 1690.
(9) Inaba, N.; Yamada, T.; Suzuki, S.; Hashimoto, T. *Macromolecules* **1988**, *21*, 407.
(10) Nakai, A.; Shiwaku, T.; Hasegawa, H.; Hashimoto, T. *Macromolecules* **1986**, *19*, 3008.
(11) Hasegawa, H.; Shiwaku, T.; Nakai, A.; Hashimoto, T. In *Dynamics of Ordering Processes in Condensed Matter*; Komura, S., Furukawa, H., Eds.; Plenum Press: New York, 1988; p 457.
(12) Kyu, T.; Zhuang, P. *Polym. Commun.* **1988**, *29*, 99.
(13) Kawanashi, K.; Komatsu, M.; Inoue, T. *Polymer* **1987**, *28*, 981.
(14) Hashimoto, T. In *Thermoplastic Elastomers, A Comprehensive Review*, 2nd ed.; Legge, N. R., Holden, G., Schroeder, H. E., Eds.; Hanser: Munich, Germany, 1996; p 429.
(15) Bates, F. S.; Fredrickson, G. H. *Annu. Rev. Phys. Chem.* **1990**, *41*, 525.
(16) Tanaka, H.; Hashimoto, T. *Polym. Commun.* **1988**, *29*, 212.

(17) Hashimoto, T.; Tanaka, H.; Hasegawa, H. In *Molecular Conformation and Dynamics of Macromolecules in Condensed Systems*; Nagasawa, M., Ed.; Elsevier: Amsterdam, The Netherlands, 1988; p 257.
(18) Hashimoto, T.; Kimishima, K.; Hasegawa, H. *Macromolecules* **1991**, *24*, 5704.
(19) Hasegawa, H.; Hashimoto, T. In *Comprehensive Polymer Science, Second Supplement*; Aggarwal, S. L., Russo, S., Eds.; Pergamon: New York, 1996; p 497.
(20) Hong, K. M.; Noolandi, J. *Macromolecules* **1983**, *16*, 1083.
(21) Roe, R.-J.; Zin, W. C. *Macromolecules* **1984**, *17*, 189.
(22) Zin, W.-C.; Roe, R.-J. *Macromolecules* **1984**, *17*, 183.
(23) Whitmore, M. D.; Noolandi, J. *Macromolecules* **1985**, *18*, 2486.
(24) Lowenhaupt, B.; Hellman, G. P. *Polymer* **1991**, *32*, 1065.
(25) Douy, A.; Mayer, R.; Rossi, J.; Gallot, B. *Mol. Cryst. Liq. Cryst.* **1969**, *7*, 103.
(26) Skoulious, A.; Helffer, P.; Gallot, Y.; Selb, J. *Makromol. Chem.* **1971**, *148*, 305.
(27) Nojima, S.; Roe, R.-J. *Macromolecules* **1987**, *20*, 1866.
(28) Owens, J. N.; Gancarz, I. S.; Koberstein, J. T.; Russell, T. P. *Macromolecules* **1989**, *22*, 3388.
(29) Tanaka, H.; Hashimoto, T. *Macromolecules* **1991**, *24*, 5398.
(30) Tanaka, H.; Sakurai, S.; Hashimoto, T.; Whitmore, M. D. *Polymer* **1992**, *33*, 1006.
(31) Quan, X.; Gancarz, I.; Koberstein, J. T.; Wignall, G. D. *Macromolecules* **1987**, *20*, 1431.
(32) Berney, C. V.; Cheng, P.-L.; Cohen, R. E. *Macromolecules* **1988**, *21*, 2235.
(33) Hashimoto, T.; Tanaka, H.; Hasegawa, H. *Macromolecules* **1990**, *23*, 4378.
(34) Winey, K. I.; Thomas, E. L. In *Material Research Society*; Schaefer, D. W., Mark, J. E., Eds.; Elsevier: New York, 1990; Vol. 171.
(35) Tanaka, H.; Hasegawa, H.; Hashimoto, T. *Macromolecules* **1991**, *24*, 240.
(36) Noolandi, J.; Hong, K. M. *Macromolecules* **1983**, *16*, 1443.
(37) Leibler, L.; Pincus, P. A. *Macromolecules* **1984**, *17*, 2922.
(38) Rigby, D.; Roe, R.-J. *Macromolecules* **1984**, *17*, 1778.
(39) Rigby, D.; Roe, R.-J. *Macromolecules* **1986**, *19*, 721.
(40) Roe, R.-J. *Macromolecules* **1986**, *19*, 728.
(41) Kinning, D. J.; Winey, K. I.; Thomas, E. L. *Macromolecules* **1988**, *21*, 3502.
(42) Witten, T. A.; Milner, S. T.; Wang, Z. G. In *Contemporary Topics in Polymer Science, Vol. 6, on Multiphase Macromolecular Systems Symposium*; Culbertson, W. M., Ed.; Plenum Press: New York, 1989.
(43) Schull, K. R.; Kramer, E. J.; Hadziioannou, G.; Tang, W. *Macromolecules* **1990**, *23*, 4780.
(44) Tanaka, H.; Hashimoto, T. *Macromolecules* **1991**, *24*, 5713.
(45) Schultz, A. R.; Beach, B. M. *J. Appl. Polym. Sci.* **1977**, *21*, 2305.
(46) Tucker, P. S.; Barlow, J. W.; Paul, D. R. *Macromolecules* **1988**, *21*, 1678.
(47) Tucker, P. S.; Barlow, J. W.; Paul, D. R. *Macromolecules* **1988**, *21*, 2794.
(48) Tucker, P. S.; Paul, D. R. *Macromolecules* **1988**, *21*, 2801.
(49) Lowenhaupt, B.; Steurer, A.; Hellman, G. P.; Gallot, Y. *Macromolecules* **1994**, *27*, 908.
(50) Hashimoto, T.; Izumitani, T.; Oono, K. *Macromol. Symp.* **1995**, *98*, 925.
(51) Lee, H.-K.; Kang, C.-K.; Zin, W.-C. *Polymer* **1996**, *37*, 287.
(52) Lee, H.-K.; Kang, C.-K.; Zin, W.-C. *Polymer* **1997**, *38*, 1595.
(53) Kimishima, K.; Hashimoto, T.; Han, C. D. *Macromolecules* **1995**, *28*, 3842.
(54) Nishi, T.; Wang, T. T.; Kwei, T. K. *Macromolecules* **1975**, *8*, 227.
(55) Snyder, H. L.; Meakin, P.; Reich, S. *Macromolecules* **1983**, *16*, 757.
(56) Hashimoto, T.; Kumaki, J.; Kawai, H. *Macromolecules* **1983**, *16*, 641.
(57) Hashimoto, T.; Suehiro, S.; Shibayama, M.; Saijo, K.; Kawai, H. *Polym. J.* **1981**, *13*, 501.
(58) Fujimura, M.; Hashimoto, T.; Kawai, H. *Mem. Fac. Eng., Kyoto Univ.* **1981**, *43* (2), 224.
(59) Suehiro, S.; Saijo, K.; Ohta, Y.; Hashimoto, T. *Anal. Chim. Acta* **1986**, *189*, 41.
(60) Hashimoto, T.; Sasaki, K.; Kawai, H. *Macromolecules* **1984**, *17*, 2812.
(61) Hashimoto, T. In *Progress in Pacific Polymer Science 2*; Imanishi, Y., Ed.; Springer: Berlin, Germany, 1992 (see Figure 13, especially).
(62) Iizuka, N.; Takenaka, M.; Hasegawa, H.; Hashimoto, T., manuscript in preparation.
(63) Matsuoka, H.; Tanaka, H.; Hashimoto, T.; Ise, N. *Phys. Rev. B: Condens. Matter* **1987**, *36*, 1754.
(64) Matsuoka, H.; Tanaka, H.; Iizuka, N.; Hashimoto, T.; Ise, N. *Phys. Rev. B* **1990**, *41*, 3854.
(65) The effects of moisture under the normal casting conditions are unavoidable. However, with the casting condition employed in this study, no macrophase separatin was observed in the as-cast films of HPS/PVME blends. It should rather be emphasized that curve b in Figure 10 is inherent to the system which contains the immiscible pair of PI and PVME. The moisture may change the relative heights of curves a and b in Figure 10.
(66) Dosho, S.; Ise, N.; Ito, K.; Iwai, S.; Kitano, H.; Matsuoka, H.; Nakamura, H.; Okumura, H.; Ono, T.; Sogami, I. S.; Ueno, Y.; Yoshida, H.; Yoshiyama, T. *Langmuir* **1993**, *9*, 394.
(67) Kotlarchyk, M.; Chen, S.-H.; Huang, J. S.; Kim, M. W. *Phys. Rev. A: At., Mol., Opt. Phys.* **1983**, *29*, 2054.
(68) Rouch, J.; Safouane, A.; Tartaglia, P.; Chen, S.-H. *J. Chem. Phys.* **1989**, *90*, 3756.
(69) Seto, H.; Schwahn, D.; Nagao, M.; Yokio, E.; Komura, S.; Imai, M.; Mortensen, K. *Phys. Rev. E: Stat. Phys., Plasma, Fluids, Relat. Interdiscip. Top.* **1996**, *54*, 629.

MA980084K